DOI 10.48011/asba.v2i1.1162

Cogging Torque Reduction by Means of Pole Segmentation Optimization on the Permanent Magnet Synchronous Machine ⋆

Hugo E. Santos, Khristian M. de Andrade Jr., Wellington M. Vilela, Geyverson T. de Paula

School of Electrical, Mechanical and Computer Engineering, Federal University of Goiás, Goiânia, GO 74605-010 BR, (e-mails: hes.ufgee@gmail.com, khristianjr11@gmail.com, wmisaelvilela@gmail.com, geyverson@gmail.com).

Abstract: One of the main obstacles during the design of permanent magnet machines consists in reducing the developed torque ripple characteristic of this type of machine. The main component of such ripples is a parasitic torque, called cogging torque. A technique present in the literature to reduce this parasitic torque considers the segmentation of the poles. This allows a decrease in the cogging torque, however reducing the air gap flux density too and thus the torque mean. Thus, in order to keep the torque mean reduction in reasonable levels, optimization techniques can be employed with the pole segmentation. The variables to be optimized are the number, distance and width of the segments. The present article proposes two methods to optimize these variables in order to minimize the cogging torque, but also maintain a satisfactory flux density value. Some constraints are added to account for the machine construction feasibility. The proposed methods were validated through a finite element analysis. The results proved the effectiveness of the proposed methods, with a reduction by up to 76% in the cogging torque and keeping, in the best case, about 95% of the reference machine air gap flux density and 78% in the worst one.

Keywords: cogging torque reduction, design optimization, pole segmentation

1. INTRODUCTION

Permanent magnet synchronous machines (PMSM) are known for their high torque density that results in a smaller volume when compared to induction motors of same rated power (Lateb et al., 2005). In addition, a PMSM have no commutation losses like the DC brushed motor (Sincero et al., 2008). However, they present a characteristic torque ripple as a disadvantage that degrades the drive performance. The cogging torque is one of the main contributors to this ripple (Abbaszadeh et al., 2011). It is caused by the tendency of the magnets and slot openings to align, resulting in a pulsating torque with zero average value. Many techniques were derived in order to reduce the cogging torque considering the machine design (Miller and Jr., 1995; Wei Hua and Ming Cheng, 2008; Breton et al., 2000; Lateb et al., 2006; Mansouri and Trabelsi, 2013; Ashabani and Mohamed, 2011; Sang-Moon Hwang et al., 2001).

The simplest technique for reducing cogging torque is based on making the appropriated choice of pole and slot numbers (Miller and Jr., 1995). However, the reduction provided is not always satisfactory and other solutions may be necessary. The skewing of the stator lamination stack or magnets in rotor produces are suited for this, but the leakage flux is increased and a reduction in the developed torque occurs (Wei Hua and Ming Cheng, 2008). Another way consists in using asymmetrical poles and slots distribution (Breton et al., 2000), increasing the complexity of the machine. There are several other techniques in the literature with their respective advantages and disadvantages. A remarkable one is the pole segmentation technique (Abbaszadeh et al., 2011; Lateb et al., 2006; Mansouri and Trabelsi, 2013; Ashabani and Mohamed, 2011) that is discussed in detail in this paper and two optimization methods for this technique are proposed.

As shown in Section II, the intensity of the cogging torque is associated to the distribution of the magnetic flux density in the air gap and the distribution of the stator slots (Lateb et al., 2006). The pole segmentation consists in dividing the poles in smaller segments. It reduces the number of alignments between the slot openings and magnets, thus reducing the cogging torque. It is a simple technique that can be applied to any size of PMSM (Abbaszadeh et al., 2011). Moreover, this technique allows a reduction in the magnets volume, but also decreases the air gap flux density. Multi-objective optimizations methods can be applied to the pole segmentation technique in order to minimize both the cogging torque and magnets volume, but keeping the flux density almost unaltered (Ashabani and Mohamed, 2011).

⋆ All the authors would like to thank CNPq, Coordenação de Aperfeiçoamento de Pessoal de Nível Superior - Brasil (CAPES) (Finance Code 001) and FAPEG (Fundação de Amparo à Pesquisa do Estado de Goiás) for funding guarantee and support.

As explained before, the usage of pole segmentation results in a decrease in the air gap flux density, and the main goal of this paper is, by means of two optimization methods, to reach a minimum cogging torque such that the motor delivers a good performance. The first condition is that the flux density does not reduce below a threshold value. Then, three machine parameters (segment number, width of segments and pole pitch) have their values changed and applied into the analytic equations shown in Section II. Their optimal value, achieved by means of an optimization process, lead to an optimal machine design that comply with low cogging torque, low torque ripple and low average torque depreciation.

This paper is divided as follows: Section II presents a detailed explanation of the pole segmentation technique, how it reduces cogging torque and the equations used in the optimization process; Sections III presents the optimization methods proposed to reduce the cogging torque; and Section IV shows the results and discussions.

2. COGGING TORQUE REDUCTION

This section presents a detailed description of the pole segmentation technique and how it is possible to reduce the cogging torque utilizing it. Equations are obtained and presented here in order to facilitate the analysis and aid the optimization process.

As the name suggests, the pole segmentation technique consists in dividing the pole in smaller segments. This can reduce the number of alignments between slot openings and magnets, thus reducing the cogging torque. An example of pole segmentation (using three segments) can be depicted in Figs. 1a and 1b.

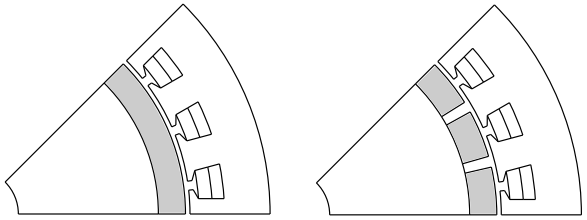

(a) Non-segmented pole (b) Segmented pole

Figure 1. Example of the pole segmentation

The air gap energy, W, variation can be considered equal to the total energy variation of the machine for a surface mounted PMSM. Thus, the cogging torque, T_C, can be obtained by differentiating W with respect to the rotor angle, α, as expressed in (1), for the no-load machine operation (Lateb et al., 2006).

$$T_C(\alpha) = -\frac{\partial W(\alpha)}{\partial \alpha} \tag{1}$$

The air gap energy may be expressed by means of its energy density, $B_g^2/2\mu_0$, being B_g the air gap flux density, V the volume of the air gap and μ_0 the permeability of free space, as can be seen in (2).

$$W(\alpha) = \int_V \frac{B_g^2}{2\mu_0} dV \tag{2}$$

It is possible to describe B_g as the scalar product of two functions. These functions are the air gap permeance function, G, and the air gap flux density function of the same machine, but without slots, B_{sl}. The first one is a modulating function in order to represent the effects of the slots. This modulating function has value equal to zero for regions under a slot opening or equal to one otherwise. Thus, (2) can be re-written as (3).

$$W(\alpha) = \frac{1}{2\mu_0} \int_V G^2 B_{sl}^2 dV \tag{3}$$

In this analysis, it is considered that leakage and fringing effects can be neglected. If the machine has non-segmented poles radially magnetized, B_{sl}^2 is constant (Wu et al., 2012). Now, for the segmented poles machine, B_{sl}^2 waveform is as shown in Fig. 2. For both cases, the G^2 waveform is as shown in Fig. 3.

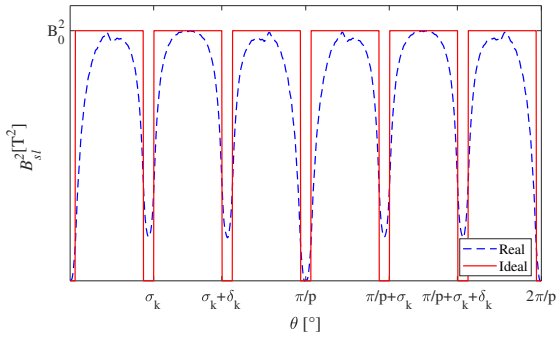

Figure 2. Real and ideal waveform of B_{sl}^2 (three segments).

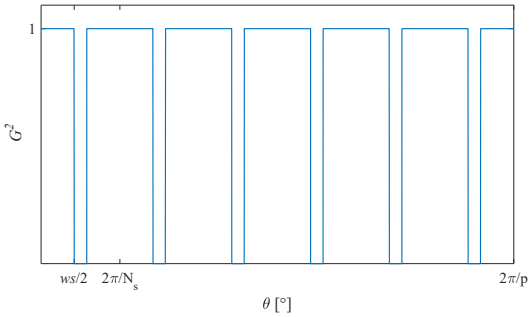

Figure 3. Ideal waveform of G^2

The functions G^2 and B_{sl}^2 may be expressed as their respective Fourier series, as (4) and (5), respectively (Lateb et al., 2006; Ashabani and Mohamed, 2011). For these equations, N_s is the slot number, p is the number of pole pairs, θ is the angular position of the air gap and m and n are positive integers.

$$G^2 = G_0 + \sum_{m=1}^{\infty} G_{mN_s} \cos(mN_s\theta) \tag{4}$$

$$B_{sl}^2 = B_{sl_0} + \sum_{n=1}^{\infty} B_{sl_{n2p}} \cos[n2p(\theta - \alpha)] \tag{5}$$

The equations (4) and (5) can be applied in (3), and then applied in (1). Using orthogonality properties, the cogging torque may be expressed as (6) (Lateb et al., 2006).

$$T_C(\alpha) = T_{C_0} \sum_{a=1}^{\infty} aN_L G_{aN_L} B_{sl_{aN_L}} \sin(aN_L\alpha) \quad (6)$$

where T_{C_0} is a parameter that depends exclusively on the machine geometry, N_L is the LCM $(N_s, 2p)$, being LCM the least common multiple, G_{aN_s} and $B_{al_{nN_L}}$ are the coefficients presented in (7) (Sang-Moon Hwang et al., 2001) and (8) (Lateb et al., 2006), respectively, and a is a positive integer.

$$G_{aN_L} = \frac{2N_s}{a\pi N_L}(-1)^{N_L/N_s} \sin(aN_L w_s) \quad (7)$$

$$B_{sl_{aN_L}} = \frac{2pB_0^2}{a\pi N_L} \sum_{k=1}^{N} \sin\left(aN_L \frac{\delta_k}{2}\right) \cos\left[aN_L\left(\sigma_k + \frac{\delta_k}{2}\right)\right] \quad (8)$$

where w_s is the angle of the teeth, B_0 is the maximum air gap flux density value, k represents the k-th segment, N is the total number of segments, σ_k is the initial angular position of a segment and δ_k is the angular width of each segment (considered equal for all segments in this work).

One can notice that in order to reduce the cogging torque without altering the machine dimensions, the coefficients G_{aN_s} and $B_{sl_{aN_L}}$ must be reduced. The pole segmentation technique allows a decrease in the $B_{sl_{aN_L}}$ coefficient, thus reducing cogging torque (Lateb et al., 2006; Ashabani and Mohamed, 2011). On the other hand, this technique also affects the first harmonic of the air gap flux density, implying in a developed torque decrease. Therefore, when using this technique, one must take special care not to greatly reduce the developed torque.

In order to verify the effects of pole segmentation technique on the air gap flux density, its Fourier series can be obtained, neglecting leakage or fringing effects, as (9). Thus, one can verify that the pole segmentation affects not only the cogging torque, but also the air gap flux, as mentioned. The air gap flux density waveform can be visualized in Fig. 4.

$$B_{sl} = B_{sl_{ip}} \sin(ip\theta) \quad (9)$$

where

$$B_{sl_{ip}} = \frac{4B_0}{i\pi} \sum_{k=1}^{N} \sin\left(ip\frac{\delta_k}{2}\right) \sin\left[ipN_L\left(\sigma_k + \frac{\delta_k}{2}\right)\right]$$

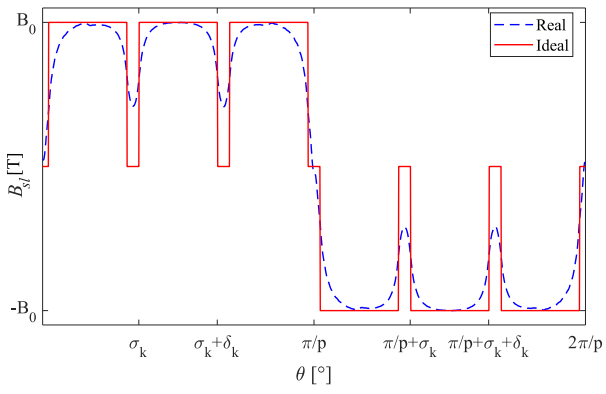

Figure 4. Real and ideal waveform of B_{sl} (three segments).

3. OPTIMIZATION

As mentioned in Section II, the fundamental of the air gap flux density, B_1, can be reduced when segmenting the poles. So, in order to reduce the cogging torque and also guarantee that B_1 will not have a great reduction, an optimization process can be employed. The methods to achieve this are described in this section.

3.1 Method I

The first method, proposed by the authors, considers (8). One can notice that in order to eliminate (ideally) a specific harmonic j, one must choose a δ_k such that $\delta_k = {}^{2\pi}/_{jN_L}$ (Lateb et al., 2006). It is noteworthy that the elimination of one harmonic does not guarantee that the minimum cogging torque is obtained. So, to minimize the cogging torque, the objective function OF_1 presented in (10) must be minimized, obtaining the optimal values of δ_k and σ_k. Also, the value of (11) must be greater or equal to a certain threshold value.

$$OF_1 = \sum_{j=1}^{11} \sum_{k=1}^{N} \sin\left(jN_L \frac{\delta_k}{2}\right) \cos\left[jN_L\left(\sigma_k + \frac{\delta_k}{2}\right)\right] \quad (10)$$

$$B_1 = \frac{4B_0}{\pi} \sum_{k=1}^{N} \sin\left(p\frac{\delta_k}{2}\right) \sin\left[pN_L\left(\sigma_k + \frac{\delta_k}{2}\right)\right] \quad (11)$$

For this paper, the optimal value of σ_k was obtained varying the pole pitch and δ_k. The distance between the segments was then calculated accordingly.

3.2 Method II

The second method that comprises a multi-objective optimization, is proposed here. Three parameters are to be optimized, being the magnets volume (V_M), a function estimating the cogging torque peak (T) varying α, as described in (12), and the fundamental of the air gap flux. There are many ways to solve multi-objectives optimization, like the "ant colony" (Guo and Zhu, 2012), "genetic algorithms" (Fonseca and J.Fleming, 1996) and "taboo search" (Baykasoglu et al., 1999). Here, the multi-objective is converted in a single objective optimization, using the objective function described in Ashabani and Mohamed (2011). This objective function, OF_2, shown in (13), must be maximized and also keeping (11) above a certain threshold.

$$T = \max\left(\sum_{a=1}^{\infty} aN_L G_{aN_L} B_{sl_{aN_L}} \sin(aN_L\alpha)\right) \quad (12)$$

$$OF_2 = \frac{B_1^2}{V_M T^3} \quad (13)$$

4. FINITE ELEMENTS ANALYSIS

The finite elements analysis was used to validate the proposed methods. Three-phase Machines with four and eight poles were considered for this analysis. Their parameters are shown in Table 1.

The machines obtained using methods I (case 1) and II (case 2) were compared to machines with non-segmented

Table 1. Parameters of the machines.

Parameter	Value
Diameter over slots [mm]	96
Stack length [mm]	102
Air gap [mm]	1
Slot opening [mm]	2
Number of poles	4, 8
Number of slots	24
Rated speed [rpm]	1500
Rated power [W]	736

full pole pitch (Ref1) and a pole pitch, β (Ref2), obtained using (14) (Lateb et al., 2006). This last pole pitch can reduce the cogging torque. Tables 2 and 3 present these pole pitch values. Ref1 was only considered here to show why it is preferable to use non-full pole pitches, such as Ref 2, to obtain lower values of cogging torque. Thus, all the comparisons made here consider Ref2 parameters as the reference ones.

$$\beta = \left(b\frac{N_s}{N_L} + 0.17 \right) \frac{2\pi}{N_s},\ b = 1,\ 2,\ \cdots \tag{14}$$

To avoid unfeasible results, some constraints were added to the optimization problems. The pole pitch value must be between the values of Ref2 and Ref1. Yet, δ_k must be greater than 12°/p and smaller than 90°/p and the distance between segments, γ, must be greater than 0.5°. The B_1 value must not be less than 0.90 T and the maximum number of segments is 10.

The obtained results are presented in Tables 2 and 3 for the 4- and 8-pole machines, respectively. One can notice that method I was the most suitable for both machines regarding the cogging torque reduction. Its reduction was by up to 71.85% for the 4-pole machine and 66.86% for the 8-pole one.

It is also possible to notice the reduction in the flux density caused by the segmentation. This reduction is by up to 13.94% and 13.31% for the 4-pole and 8-pole machines when using method I, respectively. When using method II, the reduction in the flux density was by up to 5.00% and 21.67% for the 4-pole and 8-pole machines, respectively.

Method II presented the minimum volume for the 8-pole machine, whereas method I for the 4-pole. Finally, the angle constraints were satisfied, but for the 8-pole machine the B_1 constraint value was not. This last result indicates that more accurate models for B_1 can be explored in future works.

The developed torque, T_D, reduction can be noticed from Tables 2 and 3. This reduction is essentially equal to the reduction suffered by the air gap flux density. For the 4-pole machine, the torque reduction was by up to 13.93% and 5.01% for methods I and II, respectively. For the 8-pole machine, this reduction was by up to 13.06% and 21.87% for methods I and II, respectively. Furthermore, case I presented the bests results regarding the torque ripple for both machines, since for these cases the cogging torque experienced the greatest reductions.
The cogging torque waveforms for all cases can be seen in Figs. 5a and 5b for the 4-pole and 8-pole machines, respectively. It is possible to notice the reduction of the low order harmonics achieved by methods I and II. The high order harmonics can be noticed in these waveforms by a quick comparison between the waveforms of Ref1 and Ref2.

Table 2. Results for the 4-pole machine.

Parameter	Ref1	Ref2	Case I	Case II
N	1	1	7	7
δ_k	90°	77.55°	10.71°	11.97°
γ	–	–	2.14°	0.99°
Pole pitch	90°	77.55°	87.86°	89.69°
T_C [Nm]	1.2596	1.0663	0.3002	0.3672
V_M[dm^3]	0.169	0.146	0.141	.158
B_1 [T]	1.1460	1.1200	0.9639	1.064
T_D [Nm]	4.1256	4.0336	3.4718	3.8315

Table 3. Results for the 8-pole machine.

Parameter	Ref1	Ref2	Case I	Case II
N	1	1	7	8
δ_k	45°	32.55°	5.02°	4.04°
γ	–	–	1.41°	1.69°
Pole pitch	45°	32.55°	43.59°	44.12°
T_C [Nm]	2.8367	2.1385	0.7087	1.2036
V_M[dm^3]	0.169	0.122	0.132	0.121
B_1 [T]	1.1960	1.035	0.8972	0.8107
T_D [Nm]	4.4324	3.8442	3.3421	3.0188

As for the flux density and speed normalized Back-EMF waveforms, they can be visualized in Figs. 6a and 7a for the 4-pole and 6b and 7b for the 8-pole machines, for all cases. Although the machines of the cases I and II have segmented poles, their waveforms are very similar to those of the reference machines. It is possible to notice a sag in the flux density over slot openings not present in Fig. 4 and, as a consequence, a similar pattern is also observed in the Back-EMF. This sag decreases B_1 thus the reduction of the Back-EMF and electromagnetic torque, therefore a more accurate model is needed.

Figures 8a and 8b show the waveforms of the developed torque. A sinusoidal current with a 4.68 A peak was considered. It is possible to notice the reduction of the torque average and torque ripple values. Since for both machines the cogging torque has the same order as the developed torque, the torque ripple is accentuated.

5. CONCLUSIONS

The pole segmentation is an efficient way to reduce the cogging torque of permanent magnet synchronous machine, thus also reducing the developed torque ripple. Although this technique reduces the air gap flux density, it is possible to mitigate this effect by an optimization process. In this paper, two methods for this optimization were proposed. Both methods proved to be effective in reducing the cogging torque and maintaining a flux density equal to 78.33% of the reference flux density in the worst case and 95% in the best one. Method I presented the lowest cogging torque values, allowing a reduction by up to 71.85% in its value. For future works, a combination between methods I and II may be verified.

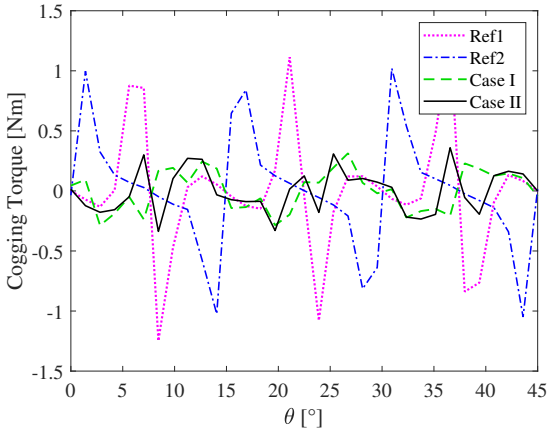

(a) Cogging torque waveform for the 4-pole machine.

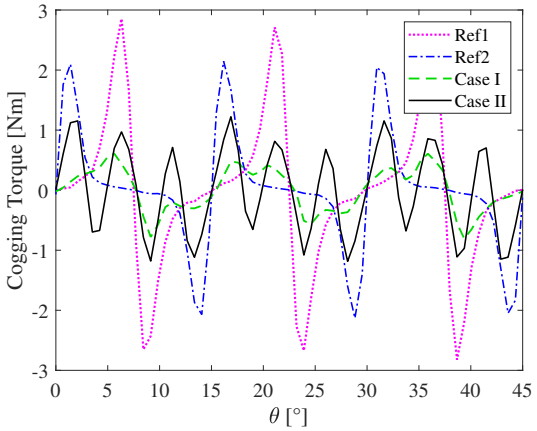

(b) Cogging torque waveforms for the 8-pole machine.

Figure 5. Cogging torque waveforms.

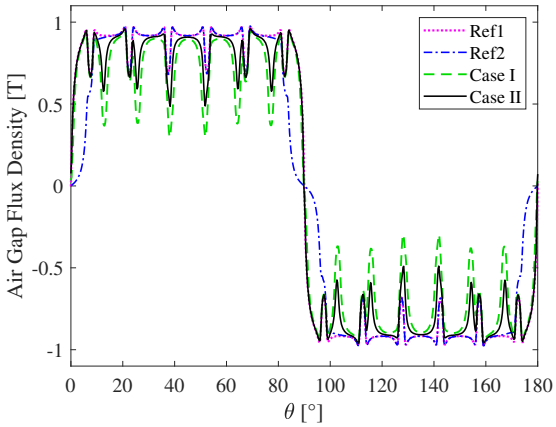

(a) Flux density waveforms for the 4-pole machine.

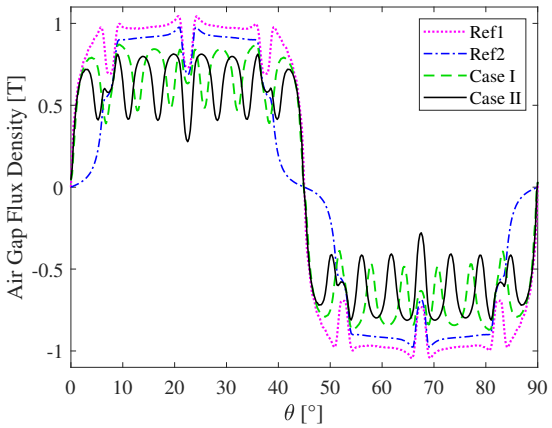

(b) Flux density waveforms for the 8-pole machine.

Figure 6. Air gap flux density waveform.

REFERENCES

Abbaszadeh, K., Alam, F.R., and Saied, S. (2011). Cogging torque optimization in surface-mounted permanent-magnet motors by using design of experiment. *Energy Conversion and Management*, 52, 3075–3082.

Ashabani, M. and Mohamed, Y.A.I. (2011). Multiobjective shape optimization of segmented pole permanent-magnet synchronous machines with improved torque characteristics. *IEEE Transactions on Magnetics*, 47(4), 795–804.

Baykasoglu, A., Owen, S., and Gindy, N. (1999). A taboo search-based approach to find the pareto optimal set in multiple objective optimization. *Engineering Optimization*, 31, 731–738.

Breton, C., Bartolome, J., Benito, J.A., Tassinario, G., Flotats, I., Lu, C.W., and Chalmers, B.J. (2000). Influence of machine symmetry on reduction of cogging torque in permanent-magnet brushless motors. *IEEE Transactions on Magnetics*, 36(5), 3819–3823.

Fonseca, C.M. and J.Fleming, P. (1996). Non-linear system identification with multiobjective genetic algorithms. *IFAC Proceedings Volumes*, 29, 1169–1174.

Guo, P. and Zhu, L. (2012). Ant colony optimization for continuous domains. In *2012 8th International Conference on Natural Computation*, 758–762.

Lateb, R., Takorabet, N., and Meibody-Tabar, F. (2006). Effect of magnet segmentation on the cogging torque in surface-mounted permanent-magnet motors. *IEEE Transactions on Magnetics*, 42(3), 442–445.

Lateb, R., Takorabet, N., Meibody-Tabar, F., Mirzaian, A., Enon, J., and Sarribouette, A. (2005). Performances comparison of induction motors and surface mounted pm motor for pod marine propulsion. In *Fourtieth IAS Annual Meeting. Conference Record of the 2005 Industry Applications Conference, 2005.*, volume 2, 1342–1349 Vol. 2.

Mansouri, A. and Trabelsi, H. (2013). Effect of the number magnet-segments on the output torque and the iron losses of a smpm. In *10th International Multi-Conferences on Systems, Signals Devices 2013 (SSD13)*, 1–5.

Miller, T.J.E. and Jr., J.R.H. (1995). *Design of Brushless Permanent-Magnet Motors*. Magna Physics Div. Tridelta Industries Inc. and Oxford University Press Inc., Hillsboro, Ohio and New York, 1 edition.

Sang-Moon Hwang, Jae-Boo Eom, Yoong-Ho Jung, Deug-Woo Lee, and Beom-Soo Kang (2001). Various de-

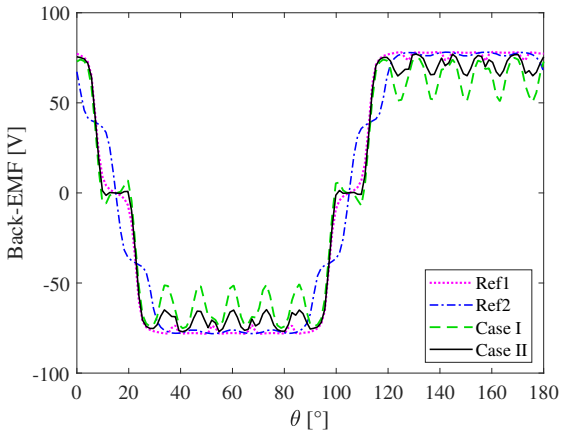

(a) speed normalized Back-EMF waveforms for the 4-pole machine.

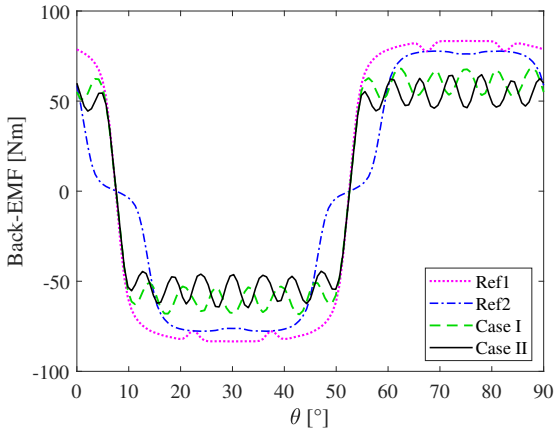

(b) speed normalized Back-EMF waveforms for the 8-pole machine.

Figure 7. speed normalized Back-EMF waveforms.

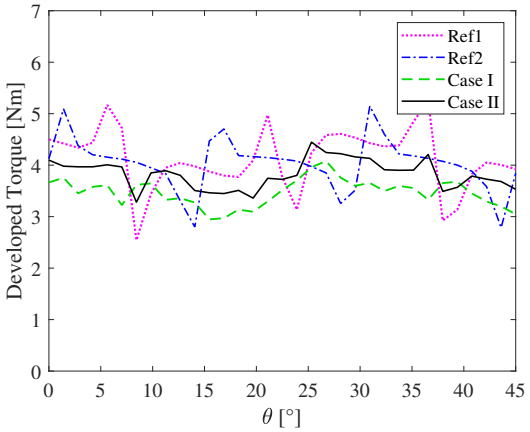

(a) Developed torque waveforms for the 4-pole machine.

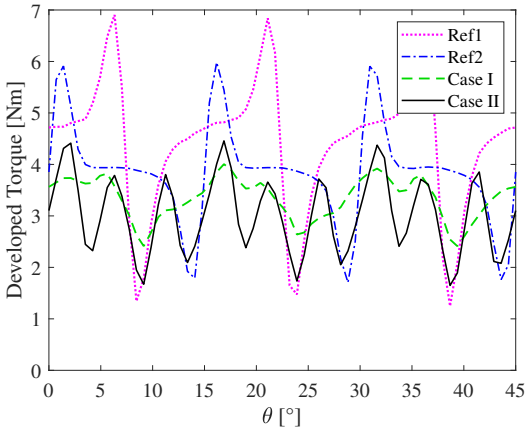

(b) Developed torque waveforms for the 8-pole machine.

Figure 8. Developed Torque.

sign techniques to reduce cogging torque by controlling energy variation in permanent magnet motors. *IEEE Transactions on Magnetics*, 37(4), 2806–2809.

Sincero, G.C.R., Cros, J., and Viarouge, P. (2008). Arc models for simulation of brush motor commutations. *IEEE Transactions on Magnetics*, 44(6), 1518–1521.

Wei Hua and Ming Cheng (2008). Cogging torque reduction of flux-switching permanent magnet machines without skewing. In *2008 International Conference on Electrical Machines and Systems*, 3020–3025.

Wu, L.J., Zhu, Z.Q., Staton, D.A., Popescu, M., and Hawkins, D. (2012). Comparison of analytical models of cogging torque in surface-mounted pm machines. *IEEE Transactions on Industrial Electronics*, 59(6), 2414–2425.